Available online at www.sciencedirect.com

ScienceDirect

Procedia Engineering 138 (2016) 403 – 412

Procedia Engineering

www.elsevier.com/locate/procedia

"SYMPHOS 2015", 3rd International Symposium on Innovation and Technology in the Phosphate Industry

Optimizing a Hydrofoil for Industrial Use

Spogis, N.[a] and Nunhez, J. R.[b]*

[a] *ESSS, Rua do Rocio, 423 10 andar conj.1001/1002, Vila Olímpia – CEP: 04552-000 – São Paulo– SP – Brazil.*
[b] *UNICAMP - Faculdade de Engenharia Química, Departamento de Engenharia de Processos, Universidade Estadual de Campinas, Cidade Universitária Zeferino Vaz, Av. Albert Einstein, 500, CEP: 13083-970 – Campinas – SP – Brazil.*

Abstract

In a previous work, Spogis and Nunhez (2009) proposed an optimization procedure for mixing tanks in which optimization methods inside modeFRONTIER were used with a computational fluid dynamics (CFD) model. The optimization software was used in conjunction with ANSYS CFX tools in order to obtain an optimal design of a high efficiency impeller for solid suspension. This procedure linking optimization methods is not new and has been used, for example, in the aerospace industry with a view to improve the shape of airplane wings (Makinen et al., 1999), in the improvement of diesel engines (Shi and Reitz, 2008) and to improve process equipment such as heat exchangers (Foli et al., 2006). Spogis and Nunhez (2009) followed the idea and proposed the use of CFD along with an optimization model for stirred tanks for the first time.

The impeller proposed in that contribution has mechanical and design problems that make it impossible for this impeller to be produced for industrial use. The power number of the impeller proposed by Spogis and Nunhez (2009) is 0.05 and the flow number is 0.2. This means that an industrial impeller, in order to pump well inside the tank needs an impeller rotating at a high speed which, in turn, can cause the impeller to work at unstable conditions. Even though the power consumption is very low, the effective flow number is also low.

An industrial impeller needs a high flow number and Power number higher than 0.2 in order to pump well at low speeds and still present a low power draw. This further refinement was implemented and, even though the procedure is similar to the one presented by Spogis and Nunhez (2009), the new impeller configurations is completely different.

[1] and [2] - Authors to whom all correspondence should be addressed.

Peer-review under responsibility of the Scientific Committee of SYMPHOS 2015

* Corresponding author. Tel.: +55 (19) 3521-3967.
E-mail address: j.r.nunhez@gmail.com

Peer-review under responsibility of the Scientific Committee of SYMPHOS 2015
doi:10.1016/j.proeng.2016.02.099

Keywords: Mixing, Solid Suspension, Computational Fluid Dynamics, Stirred Tank, Optimization, Hydrofoil

1. Introduction

Mixing vessels are widely used in the chemical, petrochemical, pharmaceutical, biotechnological and food processing industries to optimize mixing and/or heat transfer. Mixing must be efficient to ensure optimum product quality (Oldshue, 1983 and Joaquim Jr. et al., 2007, Paul et al., 2004). Variables of interest may include mixing time, gas hold-up, power draw, local shear, strain rates and solid distribution.

In this study, a new impeller for solid suspension is using a CFD approach coupled with a Multi-Objective Design Optimization method. The work follows the approach presented by Spogis and Nunhez (2009). A refinement of the work added a restriction on the power number value to ensure the proposed impeller can be used in a wider range of industrial applications.

The model consists in the creation of an environment that automatically performs the following tasks:

- Generation of the CAD design following the optimization conditions given by the mode FRONTIER software;
- Mesh generation and boundary conditions precription setup to the tank geometry and impeller design with the use of parametric automated meshing. Parametric meshing consists of giving the characteristics of the geometry and the mesh quality (including y+ and other mesh characteristics) to the ICEM mesh software which enables the automated generation of the mesh;
- CFD numerical solution;
- Estimation of the Power number, Flow number and the solid suspension using the post-processor;
- Correction of the impeller speed to guarantee same power consumption for all impeller prototypes;
- Inputting of the results to the modeFRONTIER optimization software;
- Generation of a new geometry until the group of optimum prototypes is generated.

All steps above are carried out in an automated manner. In other words, after the environment is created, the solution procedure starts and proceeds automatically until the set of optimized geometries is found.

The ANSYS CFX software was chosen for the numerical CFD results. ANSYS ICEM CFD was chosen for the Geometry and Mesh generation process in order to provide sophisticated geometry acquisition, mesh generation, mesh editing and a wide variety of solver outputs. The batch pre-processing, processing and post-processing operations were incorporated inside modeFRONTIER.

The optimization software modeFRONTIER was chosen as the optimization software because it is composed of models that range from gradient-based methods to genetic algorithms. It allowed the specification of the two objective functions used to design the impeller namely: 1 – the minimization of the concentration variance inside the vessel and 2 – the maximization of the impeller efficiency, defined by the quotient (Flow Number/Power Number). The further restriction that N_P should be higher than 0.2 is included int the model. Factors that influence the impeller geometry were also successfully investigated using this tool. This optimization software in effect became a link between the design generating tool (CAE tools) and the mesh and CFD models (ICEM and CFX) optimizing the procedure by modifying the value assigned to the input variables (design parameters and flow requirement) and monitoring the outputs. Section 2.2 explains the optimization procedure in more detail.

2. The numerical model

In the following sections, a brief description of the model is given, since this work follows the work of Spogis and Nunhez (2009).

2.1 Governing equations for fluid flow (Spogis and Nunhez, (2009))

The set of equations solved numerically by ANSYS CFX were the unsteady Navier-Stokes equations in their conservation form and the mass conservation equation. It also used the Alternate Rotation Model that solves numerically the absolute frame velocity instead of the relative velocity.

The Frozen Rotor model was used in a 120° sector of the reactor. The Shear Stress Transport (SST) turbulence

model was used since it is more accurate and robust for the prediction of problems involving flow separation.

3. Vessel parameterization

The vessel parameterization follows Spogis and Nunhez (2009) and is repeated here for convenience. A schematic representation of the vessel configuration is shown in Figure 1. The system consists of a torispherical-bottomed cylindrical vessel with diameter T and height H, which equals the height of the liquid. The off-bottom clearance is constant and equals H/4.

The torispherical 100-6 head has a crown radius of 100% (or equal to) the diameter of the head with a knuckle radius of 6% of the diameter of the head. The shaft of the impeller is concentric with the axis of the vessel. The actual geometric parameters, which are considered as a standard configuration, are summarized in Table 1 (inside Figure 1). The fluid is water at 25^0 C, with density ρ = 997.0 kg/m³ and viscosity μ= 0.8899 cP.

Parameters	Parameter Value
Tank diameter	T = 1m
Height of the liquid	H= T = 1m
Bottom clearance	C=H/4 = 0.25m

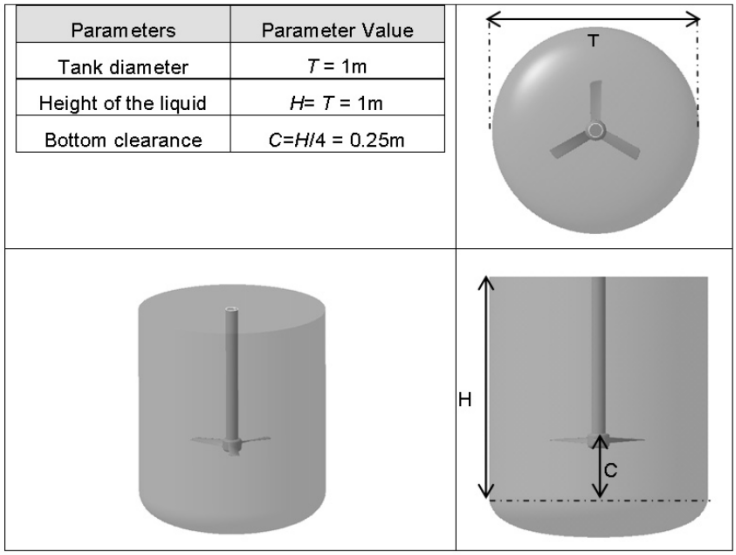

Figure 1 – Schematic representation of the stirred tank studied in this work.

4. Impeller design variables and meshing

The shape of the blades follows the work of Spogis and Nunhez (2009). As already mentioned in that paper, aerodynamic designs where analyzed to improve impeller pumping. For convenience, a schematic representation of the impeller configuration already presented by Spogis and Nunhez (2009) is repeated here and shown in Figure 2. The impeller blade design used seven construction parameters, which are even able to allow a twisting of the blade. They are:

1. Impeller diameter ratio,
2. Root chord,
3. Tip chord,
4. Root chord angle,
5. Tip chord angle,
6. Root profile,
7. Tip profile.

The root and tip profiles are two of these parameters and they are considered to be continuum variables. There are

also five are discrete variables. Table 1 shows the range of variation of these parameters. The ranges were determined based on values used for commercial impellers.

Table 1 – Impeller parameters range

Variable	Minimum Value	Maximum Value	Discrete / Continuum
Impeller diameter	0.4	0.5	Discreet
Root chord	0.2	0.2	Discreet
Tip chord	0.1	0.2	Discreet
Root chord angle	20 degrees (related to rotation axis)	70 degrees (related to rotation axis)	Discreet
Tip chord angle	30 degrees (related to rotation axis)	95 degrees (related to rotation axis)	Discreet
Root profile	DAE11, S1223, E387, FX 63-137		Continuum
Tip profile	DAE11, S1223, E387, FX 63-137		Continuum

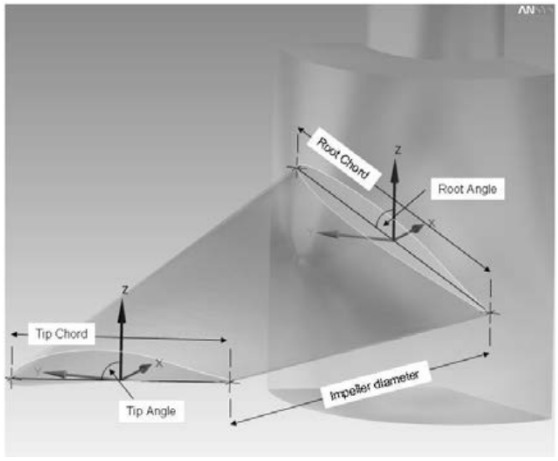

Figure 2 – Schematic representation of the impeller with the variables used in the optimization procedure

This new hydrofoil impeller was designed to maximize solid dispersion in stirred vessels at the lowest possible power consumption. The main difference to the previous work was the imposing of a lower limit of 0.2 to the Power number. Results will show the model arrived at a totally different design, when compared to the work of Spogis and Nunhez (2009). he mesh near the wall followed size restrictions. The size of the layer of control volumes near the wall are predicted by simplifications of the laminar boundary layer equations for flat plates. One of the most essential issues for the optimal performance of the SST turbulence model with curvature correction is the proper solution of the boundary layer. So the value of y+ need to be respected in order to generate meshes which satisfy the minimum requirements for accurate boundary layer computations. In order to predict turbulence correctly, it is important to have at least a layer of control volumes capturing the effect of the boundary layer, which is assessed by the dimensionless variable y^+.

A good mesh requires a minimum number of mesh points inside the boundary layer for the turbulence model to work properly. So, an estimation of the boundary layer thickness and the wall normal expansion ratio has been used in order to determine the number of nodes on the boundary layer in the direction normal to the wall.

Respecting these requirements, a hybrid (tetrahedral and prism elements) mesh was generated by the ICEM CFD tool taking the full advantage of the object oriented unstructured meshing technology. The surface mesh was generated

using the Octree approach. The volume mesh was generated by the advanced front and inflation methods and a smoothing algorithm was chosen in order to provide high element quality.

As described above it is very important to solve the boundary layer precisely on the numerical simulations. The accuracy of calculation has been improved by arranging thin prism layers near the wall. ICEM CFD Prism was used in order to generate a good prism boundary layer near the walls. The mesh generated is shown in Figure 3 (repeated for convenience from the work of Spogis and Nunhez (2009)).

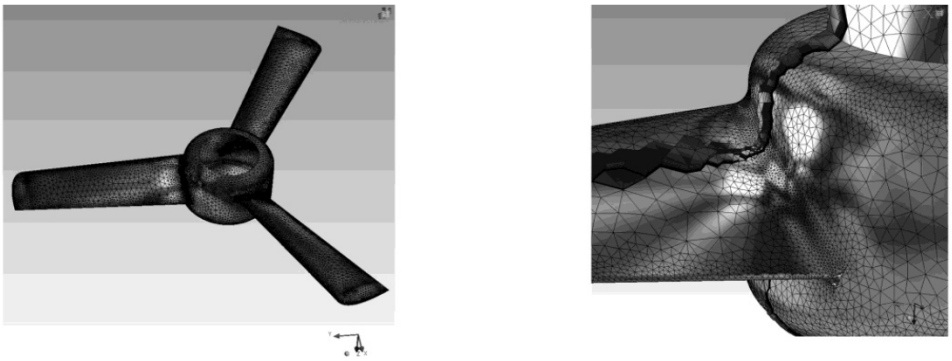

Impeller Mesh Prism Boundary Layer

Figure 3 – An example of a mesh generated in this work using adaptive meshing

5. Control program

The components described in the preceding sections are integrated and coupled into the modeFRONTIER optimization software, which is illustrated schematically in Figure 4. The control program follows the work of Spogis and Nunhez (2009) and are repeated here both for convenience and to explain the new imposing of the further restriction on the lower limit to the power number.

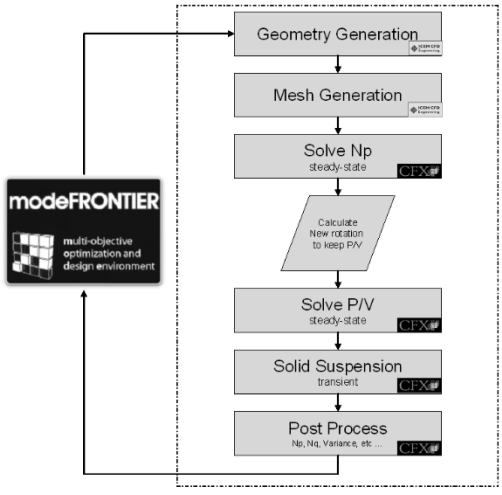

Figure 4 – Schematic Diagram of the optimization procedure

The optimization procedure involves the following major steps:

1. **Optimizer:** The optimizer is started and computes a new set of design variables. Afterward it is turned on standby.

2. **Geometry and Grid generation:** On getting the signal that the new design variables are available, the grid generation tool (ICEM CFX) becomes active and creates the new geometry and the corresponding numerical grid.
3. **Flow simulation:** Np estimation: The solver computes the flow field and estimates de Power Number – Np when it gets the signal that the new grid is available. This simulation is made using a steady state approach. The power number has the additional restriction that its value should be higher than 0.2.
4. **New rotation computation**: The value of the power number Np estimated for the geometry normally provides a power consumption different from the 2 kW/m^3 criteria chosen in this work. With the knowledge of the impeller diameter and the fluid density, a new rotational velocity is calculated in order to conserve the power consumption. Further comments of the value chosen for the power consumption are given by Spogis and Nunhez (2009).
5. **Steady state flow simulation:** With the new rotation velocity, a new steady state simulation is performed in order to determine a starting value for the next step that will determine the solid distribution. The Flow number Nq is also estimated with the new rotational speed.
6. **Transient solid dispersion:** Estimates the solid distribution within the stirred vessel.
7. **Post process results:** In this step CFX Post computes the output variables and objective functions for the new geometry, and writes them in an output ASCII file of modeFRONTIER.
8. **Test of optimizer convergence:** The optimizer decides, by the given criteria, if the current value of the objective functions should be accepted as optimum. If it is confirmed, the procedure is finished, if not, the procedure is automatically repeated from step (1).

6. Constraints

Constraint handling is an integral part of any general parameter of an optimization method. In order to restrict the solution to a limited area, only two of the defined constraints relate specifically to the creation of "realistic impeller blades" in the optimization problem:

- Tip chord angle <= Root chord angle
- Tip chord <= Root chord
- Power Number > 0.2

The angles of the root and tip chord vary, so the CAD generating model create the surface using a linear interpolation of the values of the angles starting at the hub (root chord) and finishing at the impeller tip (tip chord). The width of the blade is also an interpolation of the values of the root chord and tip chord. The final surface is obtained smoothing the lines generated by the CAD model. The constraints follow the work of Spogis and Nunhez (2009).

7. Output variables and objective functions

Ten output variables were used to monitor the mixing efficiency but only two of them were used as objective functions, which are the pumping effectiveness (quotient of the flow and power numbers) and the vessel solid concentration variance. The pumping effectiveness was maximized and the vessel solid concentration variance was minimized. These objective functions follow the work of Spogis and Nunhez (2009) and are repeated here for convenience.

The solid concentration variance of the vessel was estimated by the well known statistical formula:

$$s^2 = \frac{1}{n-1}\sum_{i=1}^{n}\left(C_i - \overline{C}\right)^2 \quad (1)$$

Were n is the number of nodes in the mixing vessel mesh. As equation 15 shows, a truly complete homogeneous solid suspension would provide $s^2 = 0$. Therefore, the optimized impeller has a low variance.

The pumping effectiveness is defined as:

$$\xi = \frac{N_q}{N_P} \quad (2)$$

The higher the pumping effectiveness is, the higher the pumping capacity will be for small power consumption.

8. Numerical results

Figure 5 shows the velocity vector plot for the design proposed by Nunhez and Spogis and Figure 6 shows the new design suggested for wider industrial use.

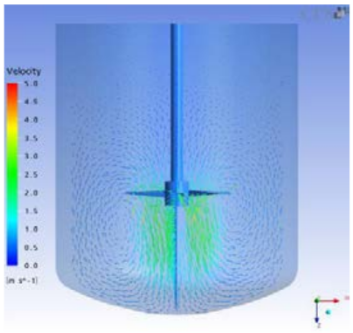

Velocity vector plot (a)

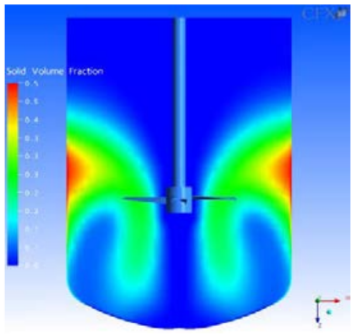

Solid distribution (b)

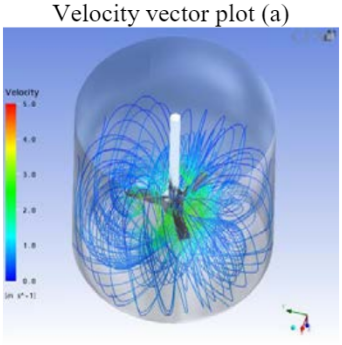

3D-Streamlines (c)

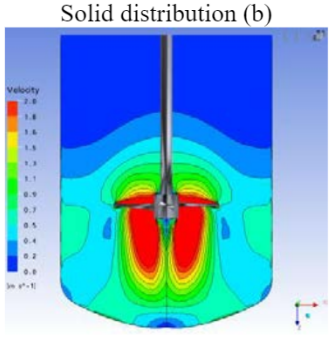

Velocity contour plot (d)

Figure 5 – Velocity, concentration and solid distribution for the design proposed by Spogis and Nunhez (2009)

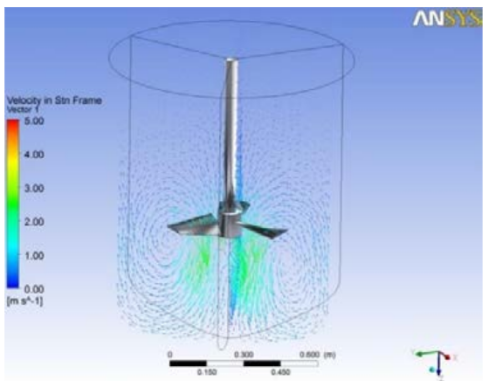

Velocity vector plot (a)

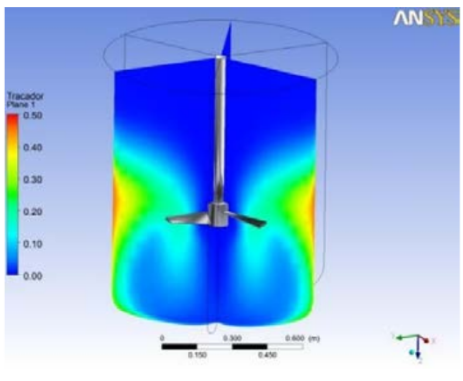

Solid distribution (b)

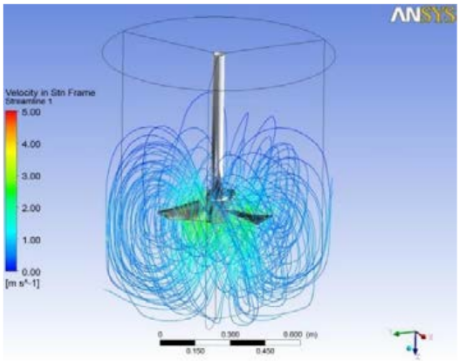

3D-Streamlines (c)

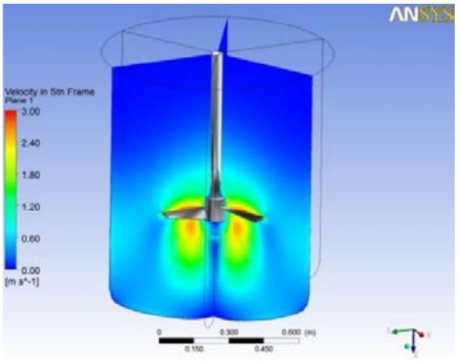

Velocity contour plot (d)

Figure 6 – Velocity, concentration and solid distribution for the Proposed Impeller for wider industrial applications

Both configurations have a very strong axial flow, resulting in higher pumping effectiveness and consequently a higher solid suspension, as shown in Figures 5b and 6b. It can be noticed that the solid concentration at the bottom of the vessel is very low, resulting in a low variance, which is the characteristic of a very well homogenized suspension. Figure 5c and 6c show the streamlines.

It can be said that the optimization procedure arrived at two impellers with a very pure axial flow. It makes sense since a pure axial flow results in a flow direction which minimizes solid settling at the bottom of the vessel. The energy is only for axial pumping, which is the objective of the work.

Figure 7a shows the impeller suggested by Spogis and Nunhez and Figure 7b the impeller proposed in this work for wider industrial use.

(a) Prototype of the geometry proposed by Spogis and Nunhez (2009)

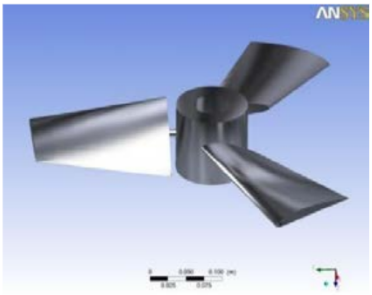

(b) New geometry proposed for wider industrial applications

Figure 7 – Optimized impellers

Table 2 compares the power number, flow number and impeller effectiveness for both configurations at turbulent flow (Re=1.00E^6).

Table 2 – Power number, flow number and impeller effectiveness.

	N_p	N_q	$\xi = N_q/N_p$
Impeller Spogis and Nunhez (2009)	0,085	0,218	2,56
Impeller for wider industrial applications	0,272	0,675	2,48

9. Experimental tests

In order to validate the CFD/Optimization model, some experimental tests were performed. Figure 8 compares the power consumption obtained by the CFD model and the experimental tank for the impeller proposed by Spogis and Nunhez (2009) and is repeated here for convenience. The results are very similar in the region where experimental results were obtained.

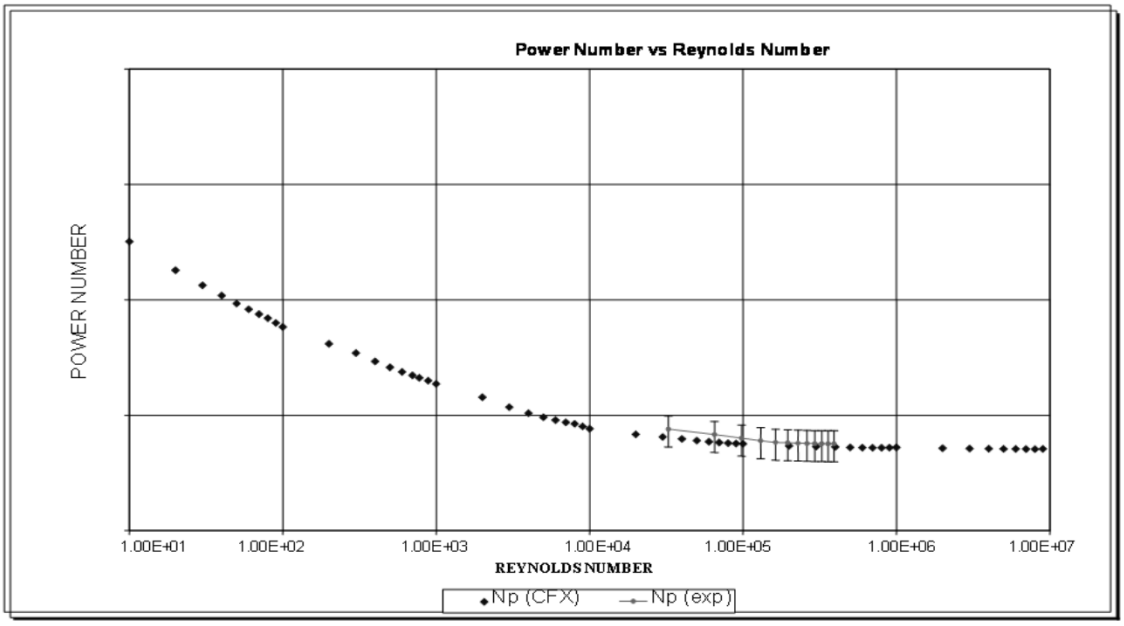

Figure 8 – Comparison between computational and experimental results

10. Summary and conclusions

This multi-objective optimization model for an optimal impeller design provided two completely different configurations that present an excellent axial flow, needed for pumping impellers. The first geometry first described by Spogis and Nunhez (2009) provided an excellent performance, but is more restricted for industrial use due very low power number. The new design proposed in this work has higher power consumption. However, it has an excellent performance compared to commercial designs and is more versatile for industrial applications when compared to the work of Spogis and Nunhez (2009).

Acknowledgements

The authors would like to thank all colleagues of ESSS and Esteco, who helped in the development of this work and also provided the software licenses used in this project, and CenPRA, that kindly manufactured the impeller prototype of Spogis and Nunhez (2009).

Notation

Throughout this article, dimensions are given in terms of the fundamental magnitudes of length (L), mass (M), time (T). This section lists symbols used in this paper, their meaning, dimensions and, where applicable, their values. Dimensionless quantities are denoted by 1. The values of physical constants (or their default values) are also given.

Nomenclature

C	Bottom clearance	[L]
D	Impeller diameter	[L]
H	Height of the liquid	[L]

N	Rotational speed	[L]
N_P	Power Number	
N_P	Pumping Number	
P	Power consumption	[W]
Re	Reynolds number	
T	Tank diameter	[L]
y^+	non-dimension distance from the wall	
ξ	impeller pumping effectiveness	
μ	Molecular (dynamic viscosity	$[M\ L^{-1}\ T^{-1}]$
ρ	Density	$M\ [L^{-3}\backslash]$
ω	Angular velocity	$[T^{-1}]$

References

[1] Foli K, Okabe T, Olhofer M, Jin YC, and Sendhoff B, Optimization of micro heat exchanger: CFD, analytical approach and multi-objective evolutionary algorithms, International Journal of Heat and Mass Transfer, 49(2006), 1090-1099

[2] Joaquim Jr, C. F.; Cekinski, E.; Nunhez, J. R. and Urenha, L. C. Agitação e Mistura na Indústria, 1 ed, LTC Editora, Rio de Janeiro, Brazil (2007).

[3] Makinen RAE, Periaux J, and Toivanen J, Multidisciplinary shape optimization in aerodynamics and electromagnetic using genetic algorithms, International Journal for Numerical Methods in Fluids, 30(1999), 149-159

[4] Menter, F.R.: Two-Equation Eddy-Viscosity Turbulence Models for Engineering Applications, AIAA Journal, Vol. 38, pp. 1598 – 1605, 1994.
modeFRONTIER: The Multi-Objective Optimization and Design Environment, http://www.esteco.it

[5] Oldshue, J. Y., Fluid Mixing Technology, 1 edition, McGraw Hill Ed., New York (1983).

[6] Patterson GK, Paul EL, Kresta SM, Etchels AW. Mixing and chemical reactions. In: Paul EL, Atiemo-Obeng VA, Kresta SM, eds. Handbook of Industrial Mixing: Science and Practice. John Wiley Sons, Inc.; 2004.

[7] Shi Y and Reitz RD, Optimization study of the effects of bowl geometry, spray targeting and swirl ratio for a heavy-duty diesel engine operated at low- and high-load, International Journal of Engine Research, 9(2008), 325-346.

[8] Spogis, N. and Nunhez, J. R. "Design of a High-Efficiency Hydrofoil Through the Use of Computational Fluid Dynamics and Multiobjective Optimization", AIChE Journal, V55, issue7, 1723-1735, (2009).